PROCEEDINGS OF ECOS 2023 - THE 36TH INTERNATIONAL CONFERENCE ON
EFFICIENCY, COST, OPTIMIZATION, SIMULATION AND ENVIRONMENTAL IMPACT OF ENERGY SYSTEMS
25-30 JUNE 2023, LAS PALMAS DE GRAN CANARIA, SPAIN

Rolling horizon Dynamic Real-Time Optimization of a solar thermal plant with a planning phase

Alix Untrau[a], Sabine Sochard[b], Frédéric Marias[c], Jean-Michel Reneaume[d], Galo A.C. Le Roux [e] and Sylvain Serra[f]

[a,b,c,d,f] Universite de Pau et des Pays de l'Adour, E2S UPPA, LaTEP, Pau, France
[a] alix.untrau@univ-pau.fr, CA, [b] sabine.sochard@univ-pau.fr, [c] frederic.marias@univ-pau.fr, [d] jean-michel.reneaume@univ-pau.fr, [f] sylvain.serra@univ-pau.fr
[e] Universidade de São Paulo, Escola Politécnica, São Paulo, Brazil, galoroux@usp.br

Abstract:
Solar thermal plants operate in a highly variable environment, with variations in both the energy source and the heat demand. Moreover, weather and load forecasts contain uncertainty. Thermal energy storage helps to decouple the heat production from the heat supply and gives the solar thermal plant more flexibility while complexifying its operation. In this work, a Dynamic Real-Time Optimization (DRTO) methodology is presented. Firstly, a planning phase determines the best storage management policy, given the estimated weather and load forecasts. An economic DRTO algorithm is then used to update the optimal trajectories to minimize the operating costs of the plant while respecting the storage management policy determined at the planning level, despite disturbances in the weather conditions. This stage uses updated forecasts and real-time information to update the optimal trajectories. This methodology is tested on a "virtual solar plant" (a detailed dynamic model of an existing plant) in a case study, with real data for the weather forecasts and measurements and a variable heat demand. Results obtained without and with DRTO adjustment are compared. In the first case, the virtual plant is operated using trajectories computed with offline dynamic optimization (DO) at the planning phase and undergoing the real-time weather and load conditions, while in the second case, real-time modification of the operating trajectories is performed. We observe an improvement in the solar fraction used to satisfy the heat demand and a reduction in the operating costs with DRTO compared to DO, without degrading the storage management significantly. The results are promising for an application to an existing plant.

Keywords:
Dynamic Real-Time Optimization, Solar thermal energy, Simulation

1. Introduction

Greenhouse gases emissions need to be reduced to mitigate climate change. An efficient energy transition is crucial to achieve carbon neutrality. Heat represents a large part of the final energy consumption and mostly relies on fossil fuels for its production nowadays. Solar thermal plants are a good alternative to fossil fuels because they allow the production of heat from the solar irradiation, and thus without direct CO_2 emissions.

1.1. Solar thermal plants challenges and opportunities

In a solar thermal plant, the solar irradiance heats up a fluid flowing through solar collectors. High temperatures, suitable for steam and electricity generation can be achieved by concentrating the solar radiation with mirrors. In the present work, we consider a non-concentrating solar thermal plant for low temperature heat production suitable for space heating, domestic hot water and some industrial processes. Nevertheless, the methodology presented in the remaining parts of the paper could be applied to other solar thermal plants. Solar energy is intermittent, with daily and seasonal variations. On the other hand, the heat demand also varies, and generally its variations are not synchronized with the variations in solar heat production. To help to decouple solar heat production and supply, Thermal Energy Storage (TES) solutions are developed. Both daily and seasonal storage solutions exist, but only daily storage is considered in this work, in the form of a stratified water tank. The association of a variable energy source and a storage solution makes the solar thermal operation complex and with several operating modes possible: direct supply, storage discharge, storage charge, shut down. Optimization methodologies are particularly promising for a system with such degrees of freedom.

1.2. Solar thermal plants optimization

Mathematical optimization is a useful tool to make the most of a system. For example, it can reduce the investment and operation costs, or the environmental impact of a system. Given the large cost of a solar thermal plant, optimizing its design and operation can help to reduce its cost and thus can improve its competitiveness

https://doi.org/10.52202/069564-0111

against fossil fuels. The design of the system, such as solar panels area, storage tank volume, etc., can be optimized to minimize the investment cost while making sure that the heat demand can be met. Once the system is designed accordingly to the consumer needs, the operation of the solar thermal plant can also be optimized in order to help to meet the heat demand despite variable weather conditions, reduce the operating cost and cut down the fossil fuel consumption in heat production.

Nowadays, most solar thermal plants are operated with logic control rules, such as a constant temperature at the outlet of the solar field, the equality of calorific fluxes in heat exchangers or the discharge of the storage tank as soon as the heat demand is not met. To track the set points determined by these logic rules, basic controllers are mostly implemented [1]. However, a solar thermal plant is a highly non-linear system, with various dynamics and ever-changing environmental conditions. Hence, more advanced controllers are developed, with predictive features for example. In the recent years, an economic objective has been incorporated in complex controllers in order to optimize the operation of systems [2]. This has been tested for a solar thermal system with storage in [3], where the back-up fossil fuel consumption was minimized. A linear control oriented model was employed to reduce the computational time since the economic optimization has to be performed at each control time step. Moreover, the control time horizon is not long enough to plan a good storage management, since the storage tank has much slower dynamics than the rest of the plant. The economic optimization and the control of the system could be performed separately to avoid the over-simplification of the dynamic model of the system.

Dynamic optimization (DO) has been applied to solar thermal plants in order to determine optimal trajectories for the control variables over a given time horizon. This is also known as planning. For example, in [4], the flow rates in the different parts of the solar thermal plant were optimized over 36 hours using weather and heat demand forecasts. In particular, the use of storage was optimized. Dynamic optimization has been more commonly applied to concentrating solar thermal plants for electricity generation. For example in [5], the income from electricity selling is maximized, with a variable electricity price and TES to shift the electricity production. A hybrid system composed of a solar thermal plant and a back up fossil fuel burner has also been optimized, in [6] for example. These studies on dynamic optimizations allowed to improve the performances of the solar thermal plants by increasing the income and reducing the back-up fossil fuel consumption. However, they relied on weather and load forecasts which are uncertain. Dynamic optimization does not adapt the optimal strategy to the current disturbances. Thus, the trajectories determined might become sub-optimal or even impossible to track by the controllers.

An intermediate level between planning and control in the hierarchical operation of the plant is real-time optimization. For a solar thermal plant, Dynamic Real-Time Optimization (DRTO) could be applied to determine the optimal trajectories of the control variables, that will be tracked by controllers [7]. These trajectories are updated regularly with a new dynamic optimization run based on updated forecasts and current measurements of state variables and disturbances. This has been tested for a concentrating solar thermal field, without considering the storage tank, in [8]. Another work focused on the daily storage management of a solar district heating system [9], by optimizing the flow rate between a long term and a short term storage tanks. These two studies only optimized in real-time a single flow rate and not the complete solar thermal plant operation, although DRTO seems well-suited to optimize such a complex system operated in an ever-changing environment.

Storage management is a particularly challenging part of the operation of a solar thermal plant. Indeed, the optimal operation of the TES has to be determined over several days, since it has slow dynamics and its optimal operation requires a long term strategic vision. However, running a new accurate dynamic optimization regularly with a time horizon of several days might lead to prohibitive computational times. A hierarchical approach might improve storage management, as shown in [10] for an electric system with storage. In this paper, a top layer is in charge of planning the storage state over a longer time horizon and a bottom layer optimizes the operation of the electric system in real-time. A similar approach could be used for a solar thermal plant, as suggested in [11]. The association of a planning phase for storage management and DRTO for the operation of the plant was only tested in one paper [16] in a theoretical case study. Reduction in the operating cost compared to DO was achieved. These promising results need to be confirmed in a more realistic case study.

Based on this literature review, there is a lack of studies focusing on the DRTO of a solar thermal plant to optimize its performances despite varying environmental conditions and consumer needs and uncertain forecasts. Moreover, a methodology to ensure a good storage management, through hierarchical optimization layers should be developed and tested in realistic case studies.

1.3. Paper contents

In the present paper, a DRTO methodology in association with a planning phase for storage management is developed. The planned storage state is incorporated into the DRTO economic objective function. The methodology is tested in a realistic case study on a simulation model. Real data are used for the weather forecasts and measurements. The test is carried out over 96 hours, showing better performances than DO without real-time adaptation.

Section 2. presents the solar thermal plant layout and its modeling. Section 3. details the input information for the algorithm. Section 4. explains the methodology with the two-layer optimization algorithm. Section 5. presents the case study chosen to test the methodology and Section 6. shows the results obtained. Finally, Section 7. gives some conclusions and perspectives for this work.

2. System description and modeling

2.1. Presentation of the solar thermal plant considered

The solar thermal plant considered in this study is presented in Fig. 1 and corresponds to an initial design of a real system provided by our industrial partner NEWHEAT. It is composed of a solar circuit, with 12 loops of 15 flat plate collectors each, where the fluid is heated up by the solar irradiation. This represents an equivalent surface of 2873m^2 of solar collectors. The fluid inside the solar circuit is composed of 70% of water and 30% of glycol in volume. The fluid can by-pass the first heat exchanger by flowing through the recirculation loop. This allows a faster warm-up of the solar circuit. Once the temperature at the outlet of the solar field is high enough for the consumer needs, the fluid flows through the heat exchanger 1, to transfer the solar heat to the secondary circuit, filled with water. The main part of the secondary circuit is a short term thermal energy storage. The technology chosen is a stratified water tank with a volume of 500m^3 and a height of 12m. The storage tank can be charged, discharged and by-passed depending on the consumer need and weather conditions. For example, the storage tank can be charged when the solar heat produced exceeds the heat demand. It can be discharged when the storage tank contains valuable energy and not enough heat is produced in the solar field. Finally, it can be by-passed to deliver directly the solar heat produced to the consumer when the heat production and demand happen simultaneously. The temperature of the fluid flowing through the second heat exchanger can be adjusted by diluting the fluid from the solar field or the storage tank with fluid exiting the second heat exchanger after having transferred its heat to the consumer. This avoids exceeding the heat demand. Three variable speed pumps are used to move the fluid in the different parts of the system and three-way valves ensure the fluid distribution in the pipes. The different operational modes of the solar thermal plant make its operation flexible but also complex. In this context, optimizing the operation of the plant should be promising because of the large number of degrees of freedom in the system. In case the heat demand is not fully satisfied by solar energy, a gas burner will be used by the consumer to reach the target temperature. The gas burner is not represented in Fig. 1 and is not modeled in our work. However, the gas consumption will be computed in order to obtain the operational cost of the heat production.

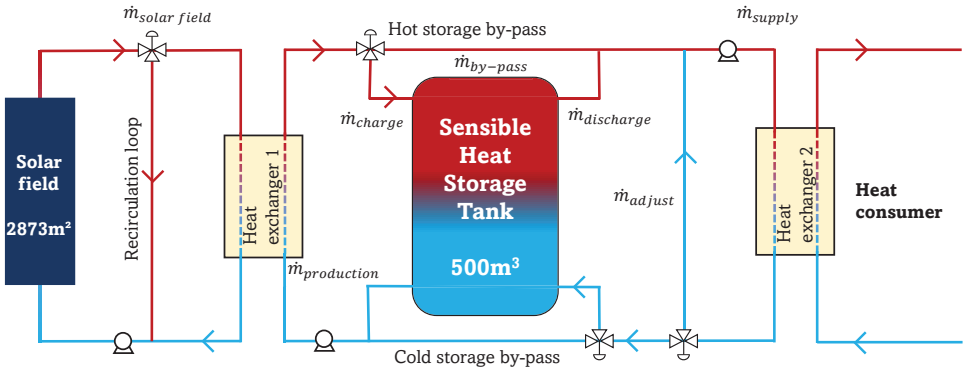

Figure 1: Solar thermal plant architecture

2.2. Modeling of the solar thermal plant

A solar thermal plant is intrinsically dynamic, with variations in the energy source and demand. The elements of the solar thermal plants have various dynamics. For instance, the solar field has fast variations while the storage tank state varies less rapidly. For these reasons, a dynamic model was chosen to represent the solar thermal plant. Moreover, nonlinear phenomena need to be represented. For example, power terms are written as the product of a flow rate and a temperature, which are both important to characterize the solar thermal plant operation. Hence, a nonlinear model was chosen. Since the optimization methodology will be tested on a simulation model, both an optimization and a simulation models are necessary. Both models are similar but some additional simplifying assumptions are made in the optimization model to keep the computational time low, as presented hereafter. The model for the solar thermal plant was developed in [4] and the main equations are detailed below, as well as some simplifying assumptions made to the original model.

https://doi.org/10.52202/069564-0111

2.2.1. Solar field

The solar field in this work is modeled as a single equivalent solar panel, with a total area A_{eq} equal to the sum of the areas of all the flat plate collectors in the solar field. The original model in [4] represented an equivalent loop of the solar field but considering a single equivalent solar panel speeds up the calculations without deteriorating the accuracy of the model significantly [12]. No spatial discretization of the collector and no heat losses between the collectors within a loop are considered. Moreover, the fluid distribution is assumed uniform between the loops. The equation modeling the solar field is the one node capacitance model written for the equivalent solar panel as follows:

$$\frac{\dot{Q}_{SF}}{A_{eq}} = \left(\eta_{0,b}(\eta_{sh} K_b(\theta) G_b + K_d G_d) - c_1(T_{mean} - T_{amb}) - c_2(T_{mean} - T_{amb})^2 - c_5 \frac{dT_{mean}}{dt} \right) \quad (1)$$

This energy conservation equation allows us to calculate the mean temperature T_{mean} inside the solar field, taking into account the heat gain from the solar irradiance, using both the direct irradiation G_b and the diffuse irradiation G_d in the plane of the collectors, the heat losses to the ambient at the temperature T_{amb} and the equivalent inertia of the collectors. $\dot{Q}_{SF}$ is the power transmitted from the sun to the heating fluid in the solar field. $\eta_{0,b}$, c_1, c_2, c_5, $K_b(\theta)$ and K_d characterize the solar collectors and are provided by the manufacturer. $\eta_{0,b}$ is the optical efficiency of the collectors, c_1 is the heat loss coefficient in the collector at $T_{mean} = T_{amb}$, c_2 is the temperature dependence of the heat loss coefficient, c_5 is the effective thermal capacity, $K_b(\theta)$ is the incidence angle modifier for the direct irradiation and K_d is the incidence angle modifier for the diffuse irradiation. η_{sh} represents the reduction in efficiency due to the shading effect. The outlet temperature of the solar field is computed assuming a linear temperature distribution in the collectors. This simplified model can represent the transient behavior of the solar field in a short computational time.

2.2.2. Storage tank

The storage tank is modeled in 1D, only the variations of the temperature along the vertical axis are considered. The storage tank is divided into N layers of same height Δz. The temperature inside each layer is assumed uniform. The energy balance can be written for each layer i, numbered from 1 at the bottom of the tank to N at the top, composed of the stored fluid and the tank wall assumed in thermal equilibrium:

$$\rho C_p A \Delta z \frac{dT_i}{dt} = US_l * (T_{amb} - T_i) + \frac{k^* A}{\Delta z}(T_{i-1} - 2T_i + T_{i+1}) + \dot{m}_{charge} C_p (T_{i+1} - T_i) + \dot{m}_{discharge} C_p (T_{i-1} - T_i) \quad (2)$$

T_i is the temperature of the layer i. The charging flux enters the top of the tank at the temperature T_{charge} and flow rate $\dot{m}_{charge}$ while the return flow enters the bottom of the tank at the temperature T_{return} and flow rate $\dot{m}_{discharge}$. C_p is the specific heat capacity of the water only because the mass of water is larger than the mass of metallic wall and the heat capacity of the metal is smaller than the heat capacity of water. ρ is the fluid density. k^* is the effective conductivity of the fluid and the tank wall, because conduction through the wall participates in destratification of the tank fluid. Heat losses between each layer and the ambient air at T_{amb} are computed with an overall heat transfer coefficient U. The exchange surface is the lateral surface of a tank layer S_l. For the top and bottom layers, the exchange surfaces and heat transfer coefficients are different than for the interior layers.

The number of layers used in the model has a great impact on the accuracy of the vertical temperature profile computed, as shown in [13] for example. The effect of numerical diffusion tends to smooth the temperature profile when a small number of layers is chosen. However, a larger number of layers increases the computational time. For the accurate simulation model used in this work to test the methodology, 1000 layers are chosen. For the optimizations, a simplified model is required to ensure reasonable computational times. Hence, only 10 layers are used, similarly to [4].

One phenomenon not represented in Eq. 2 is the natural convection. When solar irradiation goes down, at the end of the day for example, it happens that the solar heat produced is at a temperature lower than the one achieved earlier in the day. Nevertheless, its temperature is still high enough for the consumer needs. Hence, this lower temperature heat can be charged and will arrive on top of warmer stored fluid. Due to buoyancy forces, the lower temperature fluid will sink inside the tank and exchange energy with the surrounding stored fluid. This phenomenon was neglected in the optimization model for simplicity and to reduce computational time [13]. For the simulation model, the temperatures inside the tank are regularly re-organized to ensure that the top of the tank is the warmest zone and the bottom of the tank is the coldest [14].

2.2.3. Heat exchangers

The two heat exchangers are the same, both plate heat exchangers with 97 plates of 1.5m^2 each. The model used for the heat exchangers is simple to keep the computational time low: no spatial discretization, no accumulation and no heat losses are considered. The ϵ-NUT model is used to compute the exchanged energy and the two outlet temperatures. A constant global heat transfer coefficient is chosen, $U = 4000 W.m^{-2}.K^{-1}$, to reduce the nonlinearities in the model.

2.2.4. Pipes

Each pipe in the system is modeled by developing the energy balance equation in 1D without spatial discretization but considering accumulation in the fluid. Heat losses are computed with either circulating fluid or static fluid. A thermal resistance is calculated to account for external convection and conduction through the insulation layer. The external convection coefficient is computed using Hilpert correlation. Internal convection and conduction through the wall are not modeled because we assume a very large heat transfer coefficient and thus a perfect heat transfer. For the mixing valves and the flow divisions, the mass and energy balances are developed neglecting the accumulation and heat losses.

2.2.5. Pumps

Part of the operational cost of the solar thermal plant is the electricity consumption of the variable speed pumps used to move the fluid in the different circuits of the plant. First, the maximum pumping power $\dot{P}_{hydrau}$ is computed with Eq. 3, when the pressure drop in the circuit is the highest ΔP_{max}, which corresponds to the maximum flow rate allowed in the pump $\dot{m}_{max}$. Then, the actual flow rate in the circuit $\dot{m}$ is used to compute the electric power $\dot{P}_{elec}$ with the overall efficiency η_{pump} of the pump in Eq. 4.

$$\dot{P}_{hydrau} = \frac{\dot{m}_{max}}{\rho} \Delta P_{max}(\dot{m}_{max}) \quad (3) \qquad \dot{P}_{elec} = \frac{\dot{P}_{hydrau}}{\eta_{pump}} \left(\frac{\dot{m}}{\dot{m}_{max}} \right)^3 \quad (4)$$

2.2.6. Representation of the various operating modes

The complete solar thermal plant model is built by connecting the models for the solar field, storage tank, heat exchangers, pipes and pumps. The difficulty of modeling a solar thermal plant operation is the existence of various operating modes depending on the heat demand, the state of the system and the environmental conditions. Sigmoid functions are used to represent the existence of a flow in an element with a continuous formulation, allowing to neglect very small flow rates that would not be implementable in the real plant (if the flow rate is near zero, the sigmoid function is 0, otherwise it is 1). A sigmoid function is expressed as follows, with β characterizing the steepness of the function and δ the threshold:

$$sig(x) = \frac{1}{1 + exp^{-\beta(x-\delta)}} \quad (5)$$

For example, this is necessary to represent the heat exchangers through which heat can be transferred. Big M formulations are used to represent the existence of an exchanged power $\dot{Q}_{hx}$ or not, in the optimization model. If the flow rate in the heat exchanger is negligible (for example lower than $\delta = 0.5 kg.s^{-1}$), then the exchanged power is zero, otherwise it is computed with the ϵ-NUT model, with ΔT_e the difference between the inlet temperatures on each side. This is expressed as follows, with M a scalar to adjust (10^8 here) :

$$-M\ sig \leq \dot{Q}_{hx} \leq M\ sig \quad (6)$$

$$-(1 - sig)M + \epsilon(\dot{m}C_p)_{min}\Delta T_e \leq \dot{Q}_{hx} \leq (1 - sig)M + \epsilon(\dot{m}C_p)_{min}\Delta T_e \quad (7)$$

If no energy is exchanged in the heat exchanger, the outlet temperature is equal to the inlet temperature on each side. These continuous formulations allow us to represent the different working modes of the solar thermal plant. In particular, the night mode when the solar circuit is shut down and no heat is transferred in heat exchanger 1, or a mode where no solar heat is supplied to the consumer through heat exchanger 2 because the storage tank is empty and the solar irradiation is too low.

3. Input data

The study is conducted for the city of Trappes (78), France (48° 46' 39.0000" N, 2° 0' 9.0000" E). In addition to the design parameters of the system, described in Section 2., the environmental conditions and the heat demand are the inputs of the model.

3.1. Weather data

Weather forecasts as well as meteorological measurements were provided by Météo-France for the whole year of 2021 at this location. The parameters of interest are the Global Horizontal Irradiance (GHI), the Direct Normal Irradiance (DNI), the ambient temperature and the wind speed (which impacts the convection coefficient used to compute the heat losses). The weather forecasts are computed with the ARPEGE model and updated every 6 hours. Their time horizon varies depending on the run: 103h for the run at 12am, 73h for the run at 6am, 103h for the run at 12pm and 61h for the run at 6pm. Hourly values are provided for each parameter. The forecasts will be used in the optimization algorithm, to determine the best operational strategy of the solar thermal plant for a given time horizon. The same 4 parameters are measured every hour with a meteorological station. The measurements differ from the forecasts and will impact the actual solar thermal plant operation.

https://doi.org/10.52202/069564-0111

3.2. Heat demand

The consumer considered in this work is a District Heating Network (DHN) supplying heat to a residential area. In a DHN, the heat demand varies throughout the day and throughout the year. It is not easy to find available public data on the heat consumption of a DHN. Moreover, the solar thermal plant considered should be sized accordingly for the specific DHN it supplies the heat to. To simplify this case study, the same daily heat demand profile is considered for every day of the year. The real heat demand would be greater in winter than in summer due to the space heating need. The daily profile has been created in order to be consistent with the specific solar thermal plant considered. The general shape of the daily profile was retrieved from [15]. We chose that the storage tank from the solar thermal plant can supply heat to the DHN for two days when it is full. The heat demand values were then adjusted accordingly. The daily heat demand profile created is presented in Fig. 2. We observe a peak in the heat demand around 8am, and the demand is the lowest around 4pm.

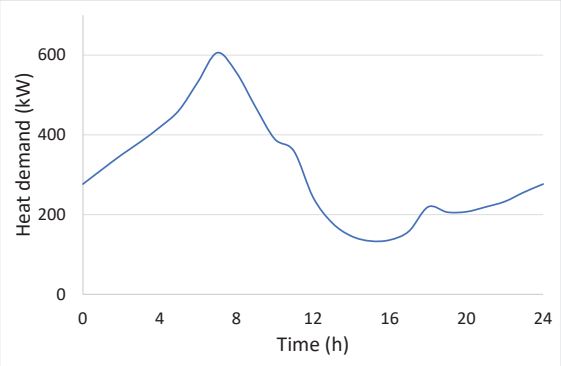

Figure 2: Daily heat demand

We consider that the DHN return temperature $T_{DHN\ return}$ is at 55°C, so the consumer inlet flow in Fig. 1 enters the heat exchanger 2 at 55°C. The target temperature T_{target} for the consumer flow after collecting the solar heat is 65°C. The flow rate of the consumer flow is variable depending on the heat demand, according to the following equation:

$$\dot{Q}_{demand} = \dot{m}_{consumer} * Cp * (T_{target} - T_{DHN\ return}) \quad (8)$$

$T_{DHN\ return}$ and $\dot{m}_{consumer}$ are both inputs of the system. The outlet temperature on the consumer side of heat exchanger 2 is calculated and should be as close as possible to T_{target} without ever exceeding it.

The variable heat demand is considered perfectly known in this work. No disturbance in the heat demand is introduced even though the methodology could be applied to an uncertain heat demand similarly to the uncertain weather conditions presented in subsection 3.1..

4. Optimization methodology

4.1. Two-level Algorithm

As explained in Section 1., the optimization methodology developed is composed of two hierarchical optimization layers to improve storage management. The methodology is tested in real-time on a simulation model, receiving the optimal trajectories and simulating the solar thermal plant actual behavior. The two-level optimization algorithm is presented in Fig. 3. The initial state of the system is that all temperatures are equal to the ambient temperature and the storage tank is half charged. The first step is the planning phase, which will be described in more details in Subsection 4.2.. It is an economic dynamic optimization that will optimize the operation of the solar thermal plant based on weather forecasts. As presented in Section 3., the longest time horizon for the weather forecasts obtained is 103 hours at 12am. Hence, the planning phase is implemented over 103 hours, starting at 0:00. The simulation model follows the optimal trajectories from the planning phase for the next 6 hours, since no weather forecast update is available. Then, the DRTO starts. Every 6 hours, a new weather forecast is available so a new DRTO is run to determine updated optimal trajectories for the next 12 hours. The DRTO economic objective function incorporates the planned storage state at the end of the DRTO time horizon. Planning is therefore used for storage management. Details on the DRTO will be provided in Subsection 4.3.. Between each DRTO run, the behavior of the system is simulated with the actual weather over the 6 hours before an update, and the simulation provides feedback to the DRTO algorithm. Details on the simulation are given in Subsection 4.4.. The complete simulation ends after 96 hours because no planned storage state is available for the next DRTO run. In a real implementation, this algorithm would be repeated continuously to optimize the operation of a solar thermal plant throughout the year, with a new planning computed regularly. In this work, the methodology was only tested for 96 hours.

4.2. Planning

The planning phase, which is an offline economic dynamic optimization follows the method developed in [4]. The degrees of freedom in the system are the 6 independent flow rates in the solar thermal plant at each time instant. The time discretization of the dynamic model for optimization is done with orthogonal collocation on

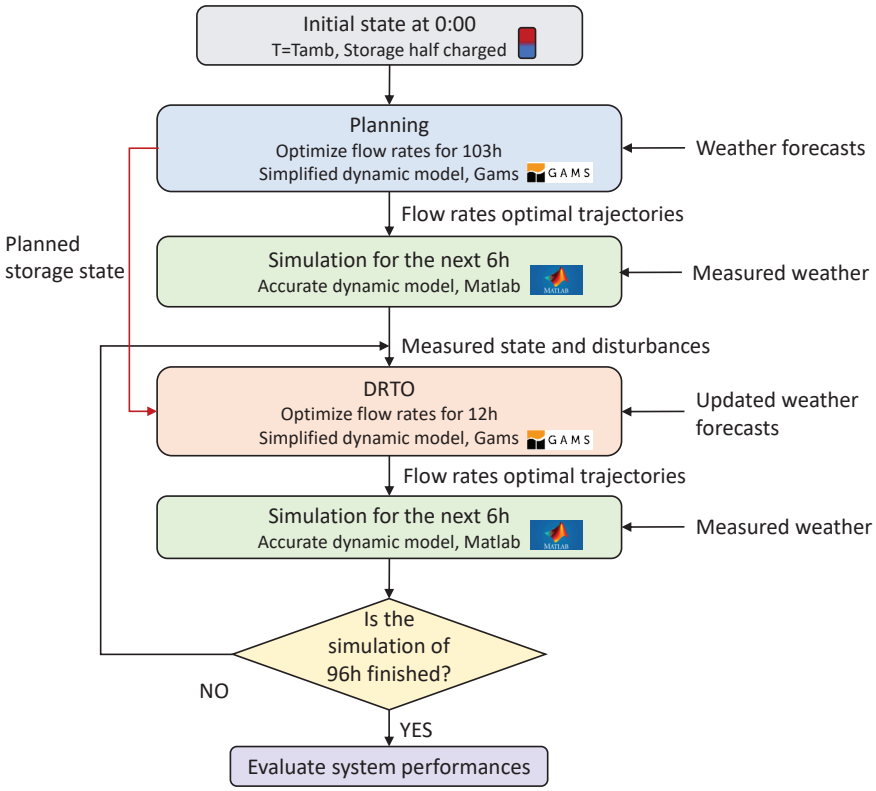

Figure 3: Two-level optimization algorithm

finite elements, with 1 hour long elements containing 9 collocation points each. The constraints in the dynamic optimization are the following:

- $T \leq 95°C$ for all temperatures T
- The flow rate in each pump is defined as follows:

$$\begin{cases} \dot{m} = 0 \text{ (corresponding to the pump turned off)} \\ \text{or} \\ 0.3\dot{m}_{max} \leq \dot{m} \leq \dot{m}_{max} \text{ (corresponding to the pump turned on, with } \dot{m}_{max} \text{ determined by the pump specifications)} \end{cases}$$

- $T_{consumer\ out} \leq T_{target}$ forbidding the heat supply to exceed the heat demand ($T_{consumer\ out}$ is the temperature of the consumer stream after collecting the solar heat)

The objective function to be minimized is the operating costs of the solar thermal plant, which are the electricity consumption of the pumps and the gas consumption of the back up burner. It includes the maximization of the stored energy at the end of the time horizon since it represents useful energy for the next hours and will allow to cut down the gas consumption. An additional term is added to smooth the trajectories obtained for the flow rates Φ_{var} and is affected by a weight γ_{var} that needs to be adjusted to achieve a good compromise between smooth flow rates trajectories and a good economic objective OF_{eco}. The formulation of the dynamic optimization problem is presented hereafter:

$$\min_{free\ \dot{m}} OF_{eco} - \gamma_{var}\Phi_{var}, \text{with} \tag{9}$$

$$OF_{eco} = -GasPrice \int_0^{t_f} \dot{Q}_{gas}(t)\mathrm{d}t - ElecPrice \int_0^{t_f} \dot{P}_{elec}(t)\mathrm{d}t + 0.7 HeatPrice\ E_{stored}(t = t_f) \tag{10}$$

The prices used are the following: *GasPrice* = 80€/MWh, *ElecPrice* = 130€/MWh and *HeatPrice* = 25€/MWh. The benefits associated to the stored energy are affected by a weight of 0.7 found appropriate in [4]. This

https://doi.org/10.52202/069564-0111

weight represents the decrease in energy quality between the moment it is stored and the moment it will be supplied. This dynamic optimization is solved with the NLP solver CONOPT in the software GAMS. The optimization is initialized with standard operating strategies ensuring that the local optimum found by CONOPT is implementable on the real plant. The planning phase takes around 2 hours to converge to an optimal solution on a laptop with the following characteristics: Intel Core i7-1065G7 1.3GHz. The stored energy throughout time determined during this planning phase will be passed to the next optimization level.

4.3. DRTO

The DRTO is also an economic dynamic optimization and is built similarly to the planning phase. Only the differences with the planning phase are presented hereafter. The time discretization is the same as planning but the time horizon is much shorter: 12 hours. With this time horizon, the methodology is applicable in real-time with a maximum computational time of 10 minutes for a DRTO on the same laptop. The economic objective function is also the same as the planning phase except for the term on the storage. In the planning phase, the stored energy at the end of the time horizon is maximized because it will be useful in the future. For the DRTO, the aim is to follow the plan established previously based on a long term strategic vision and weather forecasts. Hence, the difference between the planned stored energy and the actual storage state at the end of the DRTO time horizon is minimized. The difference is multiplied by the price of gas to obtain the order of magnitude of the cost of the non-respect of the plan, since the energy which should have been stored but was not will be replaced by gas. Finally, this term is affected by a weight ω which has been adjusted in [16] to obtain a good compromise between the following of the plan and the lowest operating costs. The value of 0.5 was chosen. This term is written as follows:

$$\omega.GasPrice.|E_{stored\ planning}(t = t_{f\ DRTO}) - E_{stored\ DRTO}(t = t_{f\ DRTO})| \quad (11)$$

Each DRTO run starts with an initial state retrieved from the simulation model, as explained in the next subsection.

4.4. Simulation

The online methodology needs to be tested on an actual plant. In this work, we replace the actual plant with a simulation performed with the solver ode15s in MATLAB. In the simulation model, perfect control is assumed so the controllers are not modeled and we assume that the optimal trajectories are perfectly tracked. The simulation model provides feedback to the DRTO algorithm. We assume that all states are measured and no state estimation step is included in the methodology. The simulation model undergoes the actual weather. It uses a more precise model for the storage tank, as explained in Subsection 2.2.2.. Since the DRTO algorithm regularly starts over with the actual system state, model error propagation due to the simplifying assumptions in the optimization model is mitigated.

5. Case study

The methodology was tested for one case study in Trappes in 2021, using the meteorological data from Météo-France. The period from the 12^{th} to the 15^{th} of May was chosen because the solar irradiance was not well predicted for this period, as shown in Fig. 4.

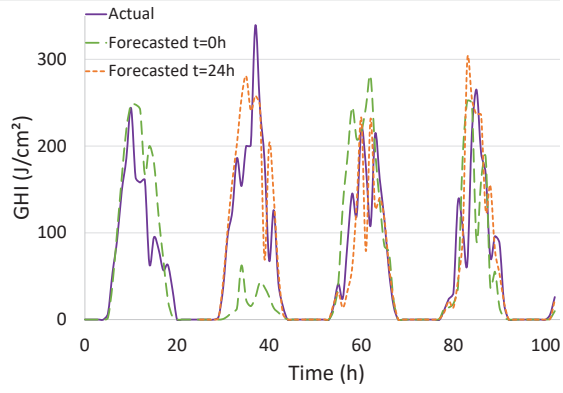

Figure 4: Predicted and actual solar irradiance for the test period in May

In this figure, the forecasted GHI plotted in dashed green line is the one used for the planning phase, at the beginning of the algorithm, while the solid purple line corresponds to the measured GHI. The solar irradiance was greatly underestimated for the second day. Forecasts are updated every 6 hours, and this underestimation is corrected in the next forecasts, which are used at the DRTO level. For example, the forecasted GHI at 24 hours is plotted in dotted orange line in Fig. 4. This forecasted GHI is closer to the measured GHI for the second day than the one predicted at 0 hours. The solar irradiation is quite variable during these four days, and the fast variations during the day are not perfectly estimated even a few hours in advance. Only the GHI was shown in Fig. 4 but a similar analysis can be conducted for the DNI.

The forecasts for the wind speed and ambient temperature are also uncertain but the differences between

forecasted values and measurements are not as large and these parameters do not impact the solar thermal plant operation as significantly as the GHI and DNI.

6. Results

6.1. Comparison between planning only and planning with DRTO

In order to assess the performances of the methodology developed, it will be compared with offline dynamic optimization (DO) without real-time adjustment, for the case study presented previously. Fig. 5 shows the comparison made.

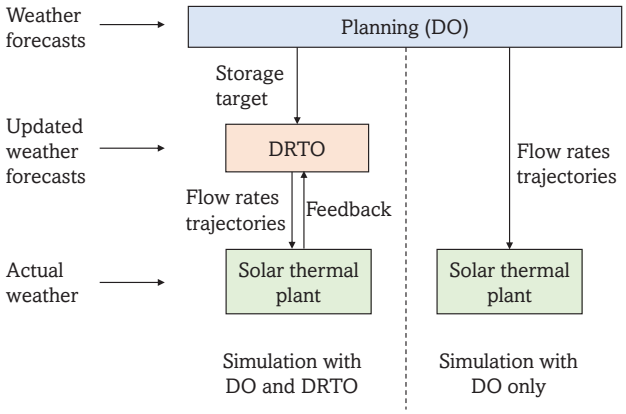

Figure 5: Comparison of simulations based on DO with DRTO and DO only

On one hand, our DRTO methodology is tested in a simulation undergoing the actual weather. The planning phase is used for storage management only, using weather forecasts. The simulation follows the optimal trajectories determined by the DRTO and regularly updated using updated forecasts. This is presented on the left side of Fig. 5. On the other hand, a simulation following the optimal trajectories determined during the planning phase (DO) is performed, with no update in the trajectories during the whole simulation undergoing the actual weather. This corresponds to the right side of Fig. 5. It was shown in the literature that offline dynamic optimization outperforms standard control strategies based on logic control rules [4]. In this section we show the interest of having real-time updates of the optimal trajectories.

6.2. Outputs

The results from the two simulations presented in the previous paragraph are compared. In Fig. 6, the flow rates in the solar field are plotted. The solid blue line corresponds to the flow rate determined during the planning phase (DO), without any update. The dash-dotted red line corresponds to the flow rate determined with our DRTO methodology. This curve is composed of sixteen portions, each six hours long, and determined by a new DRTO call. In Fig. 6, the flow rate determined by DO is zero for the second day. This is because a very low solar irradiation was predicted for that day, as shown in Fig. 4. When using our DRTO methodology, the flow rate determined during the second day is not zero because the updated weather forecasts used for the DRTO predicted a solar irradiation high enough for solar heat production. This shows that the DRTO allows the modification of the optimal trajectories when the weather forecasts are corrected.

Fig. 7 presents the temperature of the consumer stream after collecting the solar heat, $T_{consumer\ out}$, achieved for both simulations. It should be greater than the return temperature of the DHN of 55°C but lower than the target temperature of 65°C. We observe in Fig. 7 a few occurrences of a temperature lower than the DHN return temperature. This might be due to a sudden release of solar heat after a period with no supply from the source (either direct supply of from the storage). The pump is turned on but the temperature of the fluid inside the pipe has decreased due to heat losses. It takes a little time before the warm fluid reaches the second heat exchanger. There are also periods with a temperature exceeding the target temperature. For example, the temperature for DO on day 4 is much larger than 65°C. This is because the solar irradiation for this period was greatly underestimated, as shown in Fig. 4. The forecasted GHI presented a sudden decrease around hour 85 but the GHI measured actually presented a peak at that time. Hence, the operating strategy determined during planning led to exceeding the heat demand. On day 2, the solar irradiation was also greatly underestimated for the DO calculations. However, the heat demand was not exceeded on this day because the solar irradiation predicted was too low to start collecting solar heat and the storage tank was already empty at that time. Hence, the complete solar thermal plant was shut down, no solar heat was supplied and the

https://doi.org/10.52202/069564-0111

demand was thus not exceeded. However, for DRTO, the solar thermal plant was operated on day 2, delivering solar heat to the consumer. The heat demand was exceeded for part of the day because the updated forecast for the solar irradiation, although more accurate than the one used for planning and determined earlier, still underestimated the actual solar irradiation. In a real system, this behavior would be prevented thanks to local controllers forbidding to exceed the heat demand. Since our simulation model did not include controllers, nothing prevented the temperatures to go high. Adding the local controllers to our simulation model could improve the methodology before it can be tested on an actual plant. In order to avoid an optimal operating strategy that could lead to overheating, more frequent re-optimizations should be employed, based on more accurate forecasts. However, this requires access to updated forecasts very regularly. In this work, we were limited in the frequency of our DRTO runs because the weather forecasts were provided every six hours. Accurate forecasting of solar irradiation is an active area for research and new methods are developed. For example, sky imagers provide regular forecasts accounting for local clouds, or machine learning could help recomputing forecasts regularly. Figs. 6 and 7 showed that DRTO can adapt the optimal operating strategy to the actual conditions, thanks to regular re-optimizations using updated forecasts. In the next paragraph, the performances of the solar thermal plant in the two simulations are compared.

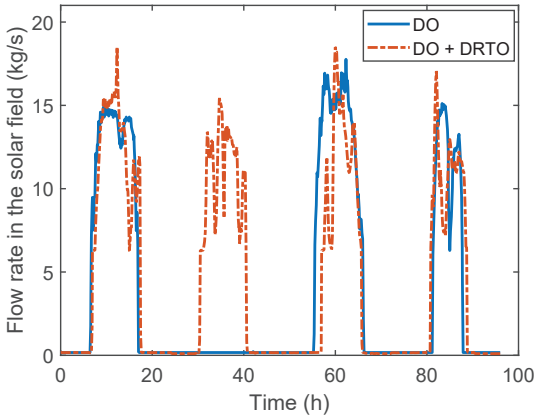

Figure 6: Comparison of the flow rates in the solar field

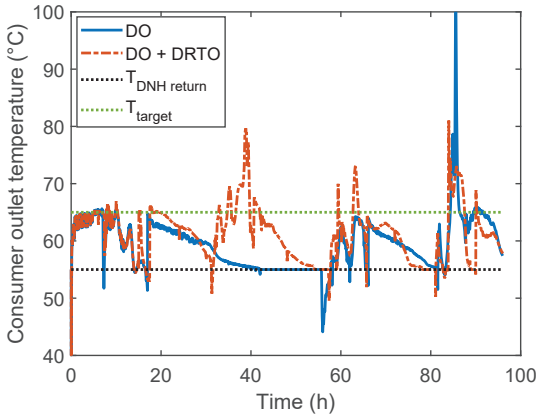

Figure 7: Comparison of the temperatures at the outlet of the consumer stream

6.3. Performances

The performances of the solar thermal plant are determined using several indicators:

- $E_{supplied}$ corresponds to the quantity of solar heat supplied at a temperature lower than the target temperature. This should be as high as possible to reduce gas consumption.
- E_{excess} corresponds to the quantity of solar heat delivered that exceeded the heat demand.
- E_{elec} corresponds to the electric consumption of the pumps.
- C_{tot} corresponds to the total operating costs of the plant (electricity and gas consumption)
- $E_{stock\ final}$ corresponds to the quantity of valuable energy inside the storage tank at the end of the simulation.

The value of each indicator for the two simulations are presented in Table 1. The total heat demand for the 96 hours of simulation is 29.8 MWh.

We observe an increase in the quantity of solar heat delivered to the consumer of about 31% with DRTO compared to DO only. This is mostly due to the solar heat supplied on the second day with DRTO, while no solar heat was produced for that day with DO. Our DRTO methodology led to more excess energy delivered in this case study, because the updated forecasts still contained inaccuracies. But this excess energy should not be delivered in a real system thanks to local controllers preventing this behavior. The electricity consumption is similar for both simulations. The total cost was reduced by 19% thanks to our DRTO methodology, because less gas was required to complete the heat demand. Finally, the quantity of energy inside the storage tank is only slightly decreased, by 1.4% of the storage capacity. However, in this case study, the storage tank is almost emptied at the end of both simulations because the solar irradiation is not very high. There is a need to study the best way to integrate storage management in the DRTO. There is probably no interest in following

Table 1: Comparison of the performances of the simulated solar thermal plant using DO only or DO+DRTO

Performance indicator	Simulation with DO only	Simulation with DO and DRTO
$E_{supplied}$ (MWh)	11.42	14.98
E_{excess} (MWh)	0.40	0.93
E_{elec} (MWh)	0.12	0.12
C_{tot} (€)	1487	1203
$E_{stock\ final}$ (MWh)	0.42	0.22

a plan determined with very inaccurate forecasts. The planning phase should be re-computed whenever the weather forecasts differ too much from the measured weather. This will be investigated in future work, with several case studies showing various levels of solar irradiation.

7. Conclusion and Perspectives

In this work, we presented a DRTO methodology using a planning phase for storage management to optimize the operation of a solar thermal plant providing heat to a DHN. The methodology was tested in a realistic case study, using real weather forecasts and measurements and a variable heat demand for four days in mid-season. The results obtained show the interest of having a real-time adaptation phase of the optimal trajectories to correct uncertainties in the weather forecasts. Thanks to DRTO, the quantity of solar heat supplied to the consumer increased, leading to a decrease in gas consumption and thus in the operating costs. The methodology developed includes the tracking of the storage state determined during the planning phase, which benefits from a better strategic vision. Thus, the DRTO is able to follow the plan while minimizing the operating costs. However, if the weather forecasts used during the planning phase are very inaccurate, following the plan is probably not optimal. A new plan should then be computed. In the mean time, a new storage management policy for the DRTO needs to be employed. Future investigations will focus on finding the best way to use the planning phase in order to improve storage management in the DRTO method. This will require testing of the methodology in various case studies.

Acknowledgments

The project leading to this publication has received funding from Excellence Initiative of Université de Pau et des Pays de l'Adour – I-Site E2S UPPA, a French "Investissements d'Avenir" programme.

Nomenclature

Abbreviations

GHI Global Horizontal Irradiance

DHN District Heating Network

DNI Direct Normal Irradiance

DO Dynamic Optimization

DRTO Dynamic Real-Time Optimization

TES Thermal Energy Storage

Latin symbols

A Tank cross sectional area, m^2

A_{eq} Area of the equivalent surface panel representing the solar field, m^2

c_1 Heat loss coefficient in the collector at $T_m = T_{amb}$, $W.m^{-2}.K^{-1}$

c_2 Temperature dependence of the heat loss coefficient, $W.m^{-2}.K^{-1}$

c_5 Effective thermal capacity, $J.m^{-2}.K^{-1}$

C_p Fluid specific heat capacity, $J.kg^{-1}.K^{-1}$

E Energy, MWh

G_b Direct irradiation (beam) in the plane of a collector, $W.m^{-2}$

G_d Diffuse irradiation in the plane of a collector, $W.m^{-2}$

k^* Effective thermal conductivity, $W.m^{-1}.K^{-1}$

$K_b(\theta)$ Incidence angle modifier for the direct irradiation (beam)

K_d Incidence angle modifier for the diffuse irradiation

$\dot{m}$ mass flow rate, kg/s

N Number of discretization layers in the storage tank

$\dot{P}$ Power, W

$\dot{Q}_{SF}$ Power transmitted from the sun to the heating fluid in the whole solar field, W

S_l Lateral surface of a tank layer, m^2

https://doi.org/10.52202/069564-0111

t Time, s

T Temperature, °C

U Tank fluid to ambient overall heat transfer coefficient, $W.m^{-2}.K^{-1}$

z Tank height from the bottom of the tank, m

Greek symbols

Δz Height of a discretization layer in the storage tank, m

ΔP Pressure drop in a circuit, Pa

$\eta_{0,b}$ Optical efficiency of a collector

η_{pump} Overall efficiency of a pump

η_{sh} Shading effect of a solar field loop onto the next loop

ρ Fluid density, $kg.m^{-3}$

References

[1] Camacho E., Rubio F., Berenguel M., Valenzuela L., *A survey on control schemes for distributed solar collector fields. Part I: Modeling and basic control approaches*. Solar Energy 2007;81:1240–1251.

[2] Engell S., *Feedback control for optimal process operation*. Journal of Process Control 2007;17:203-219.

[3] Serale G., Fiorentini M., Capozzoli A., Cooper P., Perino M., *Formulation of a model predictive control algorithm to enhance the performance of a latent heat solar thermal system*. Energy Conversion and Management 2018;173:438-449.

[4] Scolan S., Serra S., Sochard S., Delmas P., Reneaume J-M., *Dynamic optimization of the operation of a solar thermal plant*. Solar Energy 2020;198:643–657.

[5] Wittmann M., Eck M., Pitz-Paal R.,Müller-Steinhagen H., *Methodology for optimized operation strategies of solar thermal power plants with integrated heat storage*. Solar Energy 2011;85:653–659.

[6] Powell K.M., Edgar T.F, *An adaptive-grid model for dynamic simulation of thermocline thermal energy storage systems*. Energy Conversion and Management 2013;76:865-873.

[7] Kadam J.V., Schlegel M. Marquardt W., Tousain R.L., Van Hessen D.H., Van Den Berg J. Bosgra O.H., *A Two-Level Strategy of Integrated Dynamic Optimization and Control of Industrial Processes - a Case Study*. European Symposium on Computer Aided Process Engineering 2002;12:511–516.

[8] Pataro I.M.L., Roca L., Sanches J.L.G., Berenguel M., *An economic D-RTO for thermal solar plant: analysis and simulations based on a feedback linearization control case*. XXIII Congresso Brasileiro de Automatica 2020.

[9] Saloux E., Candanedo J.A., *Model-based predictive control to minimize primary energy use in a solar district heating system with seasonal thermal energy storage*. Applied Energy 2021;291:116840.

[10] Clarke W.C., Manzie C., Brear M.J., *Hierarchical economic MPC for systems with storage states*. Automatica 2018;94:138–150.

[11] Untrau A., Sochard S., Marias F., Reneaume J-M., Le Roux G., Serra S., *Analysis and future perspectives for the application of Dynamic Real-Time Optimization to solar thermal plants: A review*. Solar Energy 2022;241:275-291.

[12] Scolan S., *Développement d'un outil de simulation et d'optimisation dynamique d'une centrale solaire thermique*. Doctoral thesis, Universite de Pau et des Pays de l'Adour, Pau, France. Retrieved from https://www.theses.fr/2020PAUU3007.

[13] Untrau A., Sochard S., Marias F., Reneaume J-M., Le Roux G., Serra S., *A fast and accurate 1-dimensional model for dynamic simulation and optimization of a stratified thermal energy storage*. Applied Energy 2023;333:120614.

[14] Franke R., *Object-oriented modeling of solar heating systems*. Solar Energy 1997;60:171–180.

[15] Petkov I., Gabrielli P., *Power-to-hydrogen as seasonal energy storage: an uncertainty analysis for optimal design of low-carbon multi-energy systems*. Applied Energy 2020;274:115197.

[16] Untrau A., Sochard S., Marias F., Reneaume J-M., Le Roux G., Serra S., *Dynamic Real-Time Optimization of a Solar Thermal Plant during daytime*. Computers and Chemical Engineering 2023;172:108184.